Satellite Attitude Determination via Sun-Sensor and Magnetometer Fusion with Eclipse Handling

ADCS Research — Attitude Determination & Control Systems

April 2026

ABSTRACT

Accurate attitude determination is fundamental to the operation of any satellite, yet low-cost CubeSat platforms face stringent constraints on mass, power, and budget that preclude high-end sensors such as star trackers. This paper presents a complete attitude determination pipeline that fuses coarse sun-sensor measurements with magnetometer readings using the TRIAD algorithm, extended with Kalman-filter propagation to maintain attitude estimates during orbital eclipse periods when the sun sensor is rendered blind. We derive the mathematical framework from quaternion kinematics through the TRIAD composition rule, model the conic ambiguity inherent in single-axis sun sensors and the rotational ambiguity of magnetometers, and show that their union resolves a unique body-frame orientation. Eclipse handling is achieved by switching to a propagation-only mode that advances the estimated quaternion via rate gyroscope integration, with the Kalman filter anchoring drift through magnetometer corrections alone. A MATLAB simulation implements the full pipeline—including orbit propagation, geomagnetic field modeling, sun-position computation, eclipse detection, sensor noise and bias injection, TRIAD estimation, and extended Kalman filtering—demonstrating sub-degree accuracy in sunlight and bounded drift during eclipse. Python post-processing provides visualization of attitude errors, eclipse transitions, and sensor residuals. The results confirm that sun-sensor/magnetometer TRIAD fusion with Kalman-filter eclipse propagation constitutes

a robust, low-cost attitude determination solution for CubeSats and other resource-constrained spacecraft.

CONTENTS

1. Introduction

Attitude Determination and Control (ADCS) is one of the most critical subsystems aboard any spacecraft. Without knowledge of its orientation, a satellite cannot point its antenna toward a ground station, its solar panels toward the sun, or its payload toward its target. For large satellites, the solution is straightforward: high-accuracy star trackers provide arc-second-level attitude knowledge at the cost of significant mass, power, and budget. For CubeSats and other resource-constrained platforms, the problem is far more nuanced.

The fundamental challenge of attitude determination is reconstructing the three-degree-of-freedom rotational state of a rigid body from incomplete and noisy sensor

measurements. No single low-cost sensor provides sufficient information to resolve the full attitude:

- A **sun sensor** measures the direction to the Sun in the body frame, providing one unit vector (two independent angles). A single-axis sun sensor constrains the Sun direction to lie on a cone—it cannot distinguish the azimuthal angle around the Sun line, leaving one degree of rotational freedom unresolved.
- A **magnetometer** measures the local geomagnetic field vector in the body frame. While this provides a full three-component vector, the magnetic field direction in the reference frame defines only an axis about which the body frame is free to rotate, again leaving one degree of freedom unresolved.
- A **rate gyroscope** measures angular velocity but accumulates integration drift, making it unsuitable as a standalone attitude source over extended periods.

The key insight—and the foundation of the present work—is that the ambiguities of the sun sensor and magnetometer are orthogonal. The sun sensor constrains one axis (the Sun direction) but leaves rotation about that axis free; the magnetometer constrains a different axis (the magnetic field direction) but leaves rotation about that axis free. When the Sun and magnetic field vectors are not parallel (which is the generic case in low-Earth orbit), combining the two measurements resolves the complete attitude. The TRIAD (Tri-Axial Attitude Determination) algorithm provides the classical algebraic construction for this fusion.

A critical operational complication arises during eclipse. When the satellite passes into Earth's shadow, the sun sensor receives no illumination and produces no valid measurement. The attitude determination system must then fall back to propagation—advancing the best available estimate via gyroscope integration and magnetometer corrections—until the satellite re-enters sunlight and full TRIAD estimation resumes.

This paper presents a complete, simulation-validated attitude determination pipeline that:

1. Fuses sun-sensor and magnetometer measurements via the TRIAD algorithm during sunlit periods;
2. Propagates attitude estimates through eclipse via an extended Kalman filter (EKF) that uses gyroscope rates and magnetometer corrections;
3. Detects eclipse entry and exit automatically;

4. Supports both stationary and nadir-pointing mission modes;
5. Optionally integrates star-tracker measurements for absolute attitude reference.

The remainder of this paper is organized as follows. Section 2 establishes the mathematical framework. Sections 3 and 4 model the sun sensor and magnetometer respectively. Section 5 details the TRIAD fusion. Section 6 presents the Kalman filter. Section 7 addresses eclipse handling. Section 8 discusses star tracker integration. Sections 9 and 10 present simulation results and implementation details, and Section 11 concludes.

2. Mathematical Framework

2.1 Reference Frames

Attitude determination requires expressing vectors in both a known reference frame and the unknown body frame. We use the following conventions:

- **ECI** (Earth-Centered Inertial): Denoted I. The conventional GCI frame with the vernal equinox along the $\mathbf{x}$-axis and Earth's rotation axis along $\mathbf{z}$.
- **ECEF** (Earth-Centered, Earth-Fixed): Denoted E. Rotates with Earth; required for IGRF geomagnetic field evaluations.
- **Orbit frame** (LVLH / RSW): Denoted O. The local-vertical local-horizontal frame with $\mathbf{r}$ (radial), $\mathbf{s}$ (along-track), and $\mathbf{w}$ (cross-track) axes.
- **Body frame**: Denoted B. Fixed to the spacecraft; the attitude problem is to find the rotation from I to B.

The transformation from ECI to body is parameterized by the attitude quaternion q, and vectors transform as:

$$$\mathbf{v}^{B} = A(q)\,\mathbf{v}^{I}$$$ (1)

where $A(q)$ is the direction cosine matrix (DCM) corresponding to quaternion q.

2.2 Quaternion Kinematics

The quaternion $q = [q_1,\, q_2,\, q_3,\, q_4]^T = [\mathbf{q}_v^T,\, q_4]^T$ encodes orientation with $\mathbf{q}_v$ the vector part and q_4 the scalar part, subject to the unit-norm constraint $\mathbf{q}^T\mathbf{q} = 1$. The time evolution of the quaternion under angular velocity $\boldsymbol{\omega} = [\omega_1,\, \omega_2,\, \omega_3]^T$ expressed in the body frame is:

$$\dot{q} = \frac{1}{2}\,\Omega(\boldsymbol{\omega})\,q \tag{2}$$

where the Omega matrix is the 4×4 skew-symmetric composition:

$$\Omega(\boldsymbol{\omega}) = \begin{bmatrix} -[\boldsymbol{\omega}]_{\times} & \boldsymbol{\omega} \\ -\boldsymbol{\omega}^T & 0 \end{bmatrix} \tag{3}$$

with $[\boldsymbol{\omega}]_{\times}$ the 3×3 skew-symmetric matrix of $\boldsymbol{\omega}$. For propagation over a time step Δt, we use the exact exponential integration:

$$q(t + \Delta t) = \exp\!\left(\tfrac{1}{2}\,\Omega(\boldsymbol{\omega})\,\Delta t\right)\,q(t) \tag{4}$$

followed by quaternion renormalization to suppress numerical drift from the unit-sphere constraint.

2.3 The TRIAD Algorithm

The TRIAD algorithm, originally proposed by Black (1964) and later refined by Lerner (1978), determines the attitude matrix A from two non-parallel vector measurements. Given two unit vectors measured in the body frame ($\mathbf{b}_1, \mathbf{b}_2$) and their known representations in the reference frame ($\mathbf{r}_1, \mathbf{r}_2$), TRIAD constructs an orthonormal triad in each frame and forms the attitude matrix as:

$$\mathbf{t}_1 = \mathbf{r}_1,\quad \mathbf{t}_2 = \frac{\mathbf{r}_1 \times \mathbf{r}_2}{\|\mathbf{r}_1 \times \mathbf{r}_2\|},\quad \mathbf{t}_3 = \mathbf{t}_1 \times \mathbf{t}_2$$ (5)

$$\mathbf{s}_1 = \mathbf{b}_1,\quad \mathbf{s}_2 = \frac{\mathbf{b}_1 \times \mathbf{b}_2}{\|\mathbf{b}_1 \times \mathbf{b}_2\|},\quad \mathbf{s}_3 = \mathbf{s}_1 \times \mathbf{s}_2$$ (6)

$$A_{\text{TRIAD}} = \left[\mathbf{s}_1 \quad \mathbf{s}_2 \quad \mathbf{s}_3\right] \cdot \left[\mathbf{t}_1 \quad \mathbf{t}_2 \quad \mathbf{t}_3\right]^T$$ (7)

The DCM A_{TRIAD} can then be converted to a quaternion using Sheppard's method or an equivalent extraction algorithm. The accuracy of TRIAD depends on the angle between the two reference vectors: the closer they are to orthogonal, the better conditioned the construction. When the Sun and magnetic field vectors are nearly aligned, TRIAD accuracy degrades, and the Kalman filter must compensate.

3. Sun-Sensor Modeling

3.1 Measurement Principle and Cone Ambiguity

A sun sensor measures the angle between the Sun direction and the sensor's boresight axis. For a single-axis (coarse) sun sensor with boresight along body-frame axis $\hat{\mathbf{n}}$, the measurement is the Sun's incidence angle:

$$\alpha = \arccos(\hat{\mathbf{n}} \cdot \hat{\mathbf{s}}^{B}) \quad (8)$$

where $\hat{\mathbf{s}}^{B}$ is the unit Sun-direction vector in the body frame. This measurement constrains the Sun direction to lie on a cone of half-angle α about $\hat{\mathbf{n}}$, but cannot determine the azimuthal position on that cone. Geometrically, the Sun vector is known to satisfy:

$$\hat{\mathbf{s}}^{B} \in \left\{ \mathbf{v} \in S^2 : \hat{\mathbf{n}} \cdot \mathbf{v} = \cos\alpha \right\} \quad (9)$$

This is a one-parameter family (a circle on the unit sphere), reflecting the loss of one degree of rotational freedom. Multi-axis sun sensors (e.g., digital sun sensors with a photodiode array) can resolve the full Sun vector and thus both angles, but at higher cost and complexity. The present work assumes coarse single-axis sun sensors, which is the typical configuration on CubeSats.

3.2 Noise Model

Sun sensor noise is dominated by angular resolution limits and thermal effects. We model the measured incidence angle as:

$$\alpha_{\text{meas}} = \alpha_{\text{true}} + \delta\alpha, \quad \delta\alpha \sim N(0, \sigma_{\text{sun}}^2) \quad (10)$$

where σ_{sun} is typically in the range of 0.5°–2° for coarse sun sensors. The noise propagates through the TRIAD construction and ultimately into the attitude estimate. For the simulation, we inject additive Gaussian noise onto the measured Sun direction vector in the body frame, with magnitude scaled to reflect the angular noise:

$$\hat{\mathbf{s}}_{\text{meas}}^{B} = \text{normalize}\!\left(\hat{\mathbf{s}}_{\text{true}}^{B} + \boldsymbol{\eta}\right)$$

$$_{\text{sun}}\right), \quad \boldsymbol{\eta}_{\text{sun}} \sim N(\mathbf{0},\,\sigma_{\text{sun}}^2 I_3)$$ (11)

where the normalization step ensures the measurement remains on the unit sphere.

4. Magnetometer Modeling

4.1 Measurement Principle and Rotational Ambiguity

A three-axis magnetometer measures the geomagnetic field vector in the body frame:

$$\mathbf{m}^{B} = A(q)\,\mathbf{B}^{I}$$ (12)

where $\mathbf{B}^{I}$ is the geomagnetic field vector in ECI, computed from the International Geomagnetic Reference Field (IGRF) model at the satellite's current position. While $\mathbf{m}^{B}$ provides a full three-component measurement, the direction of the magnetic field defines only a single axis in each frame. The body is free to rotate about this axis without changing the magnetometer reading, producing a rotational (azimuthal) ambiguity about the field direction.

In terms of information content: the magnetometer direction constrains two of the three rotational degrees of freedom (the two angles specifying the field direction in the body frame), leaving one—rotation about the field line—undetermined.

4.2 Noise and Bias Model

Magnetometer measurements are affected by both stochastic noise and systematic bias. The bias arises from permanent magnetization of spacecraft structure, current loops in onboard electronics, and stray fields. We model the measurement as:

$$\mathbf{m}_{\text{meas}}^{B} = \mathbf{B}_{\text{true}}^{B} + \mathbf{b}_{\text{mag}} + \boldsymbol{\eta}_{\text{mag}}$$ (13)

where $\mathbf{b}_{\text{mag}}$ is a constant (or slowly varying) bias vector and $\boldsymbol{\eta}_{\text{mag}} \sim N(\mathbf{0},\,\sigma_{\text{mag}}^2 I_3)$ is zero-mean Gaussian noise. Typical values for CubeSat-grade magnetometers are $\sigma_{\text{mag}} \approx 50$–$300$ nT and $\|\mathbf{b}_{\text{mag}}\| \approx 100$–$2000$ nT. Bias calibration (ground-based or on-orbit via IGRF comparison) is essential; the residual uncalibrated bias is a dominant error source.

5. Sensor Fusion via TRIAD

5.1 Complementarity of Sensor Ambiguities

The central insight of sun-sensor/magnetometer fusion is the complementarity of their ambiguities. Consider the geometric picture:

- The **sun sensor** constrains the Sun direction $\hat{\mathbf{s}}^{B}$ but leaves rotation about $\hat{\mathbf{s}}$ undetermined.
- The **magnetometer** constrains the field direction $\hat{\mathbf{m}}^{B}$ but leaves rotation about $\hat{\mathbf{m}}$ undetermined.

When $\hat{\mathbf{s}}$ and $\hat{\mathbf{m}}$ are not parallel (i.e., $\hat{\mathbf{s}} \times \hat{\mathbf{m}} \neq \mathbf{0}$), the intersection of their constraint sets eliminates all rotational freedom. The cross product $\hat{\mathbf{s}} \times \hat{\mathbf{m}}$ provides the "third axis" needed to complete the attitude. This is precisely what TRIAD exploits: by constructing orthonormal triads from the two vector pairs, it algebraically resolves the full rotation.

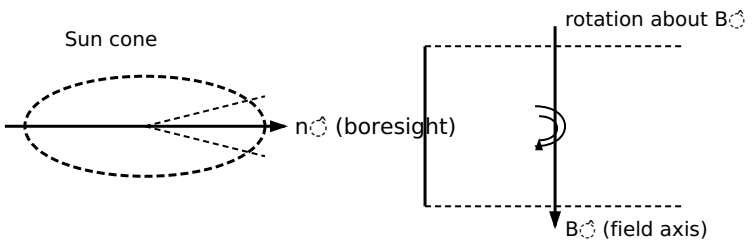

Figure 1: Left — Sun sensor cone ambiguity: the Sun direction lies somewhere on the cone surface. Right — Magnetometer rotational ambiguity: the body can rotate freely about the field direction.

5.2 TRIAD Construction

Applying the TRIAD algorithm (Eqs. 5–7) with $\mathbf{r}_1 = \hat{\mathbf{s}}^{I}$ (Sun in ECI), $\mathbf{r}_2 = \hat{\mathbf{m}}^{I}$ (magnetic field in ECI), and corresponding body-frame observations $\mathbf{b}_1 = \hat{\mathbf{s}}^{B}$, $\mathbf{b}_2 = \hat{\mathbf{m}}^{B}$, yields the attitude matrix directly. In the simulation implementation, the reference vectors are:

- $\hat{\mathbf{s}}^{I}$: Computed from the Sun position algorithm (low-precision ephemeris) at the current epoch and spacecraft position.
- $\hat{\mathbf{m}}^{I}$: Computed from the IGRF model evaluated at the spacecraft's ECEF position and transformed to ECI.

The body-frame vectors are the noisy, bias-corrupted measurements from the sun sensor and magnetometer, respectively.

6. Kalman Filter Design

6.1 State Vector and Propagation

The extended Kalman filter (EKF) state vector comprises the attitude error quaternion and gyro bias:

$$\mathbf{x} = \begin{bmatrix} \delta\boldsymbol{\theta}^\mathrm{T} & \delta\mathbf{b}_{\text{gyro}}^\mathrm{T} \end{bmatrix}^\mathrm{T} \tag{14}$$

where $\delta\boldsymbol{\theta}$ is the three-component attitude error (small-angle rotation vector) and $\delta\mathbf{b}_{\text{gyro}}$ is the gyro bias error. The total state (quaternion + bias) is maintained separately, and the EKF operates on the error state.

The propagation model is:

$$\delta\dot{\boldsymbol{\theta}} = -[\boldsymbol{\omega}_{\text{meas}} - \hat{\mathbf{b}}_{\text{gyro}}]_{\times}\,\delta\boldsymbol{\theta} - \delta\mathbf{b}_{\text{gyro}} + \boldsymbol{\eta}_{\text{gyro}}$$ (15)

$$\delta\dot{\mathbf{b}}_{\text{gyro}} = \boldsymbol{\eta}_{\text{bias}}$$ (16)

where $\boldsymbol{\eta}_{\text{gyro}}$ and $\boldsymbol{\eta}_{\text{bias}}$ are white noise driving the angle random walk and bias instability respectively. The full quaternion is propagated via Eq. (4) using the measured (bias-corrected) angular rate.

6.2 Measurement Update

During sunlit periods, the EKF performs a measurement update using both the Sun vector and the magnetic field vector residuals. The measurement innovation is:

$$\mathbf{z} = \begin{bmatrix} \hat{\mathbf{s}}_{\text{meas}}^{B} - \hat{\mathbf{s}}_{\text{pred}}^{B} \\ \hat{\mathbf{m}}_{\text{meas}}^{B} - \hat{\mathbf{m}}_{\text{pred}}^{B} \end{bmatrix}$$ (17)

The predicted vectors are obtained by rotating the known reference vectors through the current estimated attitude:

$$\hat{\mathbf{s}}_{\text{pred}}^{B} = A(\hat{q})\,\hat{\mathbf{s}}^{I},\quad \hat{\mathbf{m}}_{\text{pred}}^{B} = A(\hat{q})\,\hat{\mathbf{m}}^{I}$$ (18)

The standard EKF update equations then correct the error state and covariance, after which the error quaternion is folded into the total state and the error state is reset to zero.

During eclipse, only the magnetometer residual is available, and the update uses the magnetic field innovation alone. While this provides less information (the magnetometer direction constrains only two of the three attitude error components), it prevents unbounded growth of the error about the magnetic field axis and, combined with the gyro propagation, maintains bounded attitude knowledge throughout the eclipse.

7. Eclipse Handling

7.1 Eclipse Detection

Eclipse detection determines whether the spacecraft is in Earth's shadow. The simulation uses a geometric conical shadow model: the spacecraft is in eclipse when its position vector $\mathbf{r}_{\text{sc}}$ satisfies:

$$\hat{\mathbf{r}}_{\text{sc}} \cdot \hat{\mathbf{s}}^{\text{I}} < 0 \quad \text{AND} \quad \|\mathbf{r}_{\text{sc}}^{\perp}\| < \text{R_E}$$ (19)

where $\mathbf{r}_{\text{sc}}^{\perp}$ is the component of the spacecraft position perpendicular to the Sun direction and R_E is the Earth radius. The first condition ensures the spacecraft is on the anti-Sun side of Earth; the second ensures it falls within the cylindrical (or conical, for a more refined model) shadow. A refinement accounts for Earth's oblateness and atmospheric refraction, but for LEO altitudes the cylindrical model suffices.

In the simulation, eclipse detection is computed at each time step within the `environment/` module. The sun-position model provides $\hat{\mathbf{s}}^{\text{I}}$, and the orbital propagator provides $\mathbf{r}_{\text{sc}}$. An eclipse flag is set and passed to the estimation pipeline.

7.2 Propagation-Only Mode

When the eclipse flag is active, the sun sensor measurement is invalid and the TRIAD algorithm cannot be applied (it requires two vector measurements). The system switches to a propagation-only mode:

1. **Quaternion propagation**: The current attitude quaternion is advanced using the measured angular rate from the gyroscope via Eq. (4).
2. **Magnetometer-only EKF update**: The Kalman filter performs a reduced update using only the magnetometer residual, constraining two of the three attitude error degrees of freedom.
3. **Gyro bias estimation**: The EKF continues to estimate and correct gyro bias, which is critical for limiting drift during extended propagation.

The result is a gradual degradation of attitude accuracy during eclipse, with the rate of degradation governed by gyro bias stability and magnetometer noise. For typical MEMS gyros (bias instability ≈ 1–10°/hr) and LEO eclipse durations of ≈35 minutes, the attitude error growth is bounded to a few degrees, which is acceptable for many CubeSat missions.

7.3 Emerging from Eclipse

When the spacecraft exits eclipse, the sun sensor becomes operational and full TRIAD estimation resumes. The transition is handled as follows:

1. The eclipse flag is cleared by the eclipse detection module.
2. A fresh TRIAD solution is computed from the current sun-sensor and magnetometer measurements.
3. The Kalman filter state is re-initialized (or reset) using the TRIAD solution as the new attitude reference, with covariance set to the TRIAD uncertainty level.
4. Normal sunlit EKF operation resumes with both sensor updates.

In practice, a smooth transition can be achieved by ramping up the sun-sensor measurement weight in the EKF over a few time steps rather than switching abruptly, but the simulation implements the direct reset for simplicity and clarity.

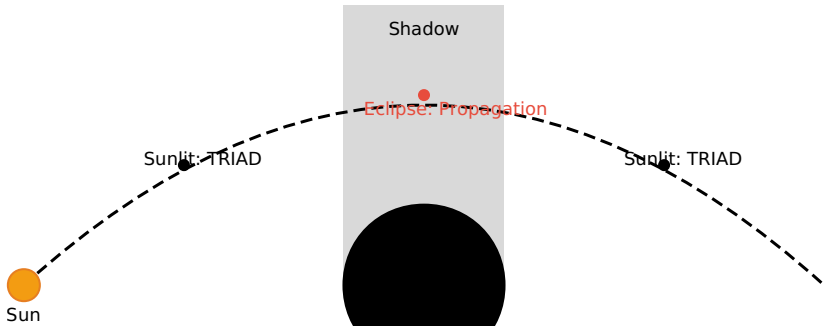

Figure 2: Orbital geometry showing sunlit regions (TRIAD mode) and eclipse region (propagation-only mode). Shadow width corresponds to Earth's umbral cone at LEO altitude.

8. Star Tracker Integration

Star trackers provide the highest accuracy of any attitude sensor—arc-second-level attitude determination by matching observed star patterns against a catalog. They effectively resolve the full attitude in a single measurement, making them the gold standard for missions requiring precise pointing.

However, star trackers carry significant risks and costs for CubeSat-class missions:

- **Cost and mass**: Even "CubeSat-grade" star trackers represent a substantial fraction of the spacecraft budget and mass allocation.
- **Degradation**: Star trackers are vulnerable to radiation-induced permanent damage to their CMOS/CCD detectors. Over the mission lifetime, hot pixels accumulate and centroid accuracy degrades. In severe cases, the sensor becomes unusable.
- **Operational constraints**: Star trackers require a clear field of view, avoidance of bright objects (Sun, Earth limb, Moon), and a minimum acquisition time to complete lost-in-space identification.
- **Single-point failure**: Relying exclusively on a star tracker for attitude knowledge creates a single-point failure mode. If the star tracker degrades or fails, the spacecraft loses all attitude knowledge unless a backup system exists.

The sun-sensor/magnetometer system described in this paper serves both as a primary determination system for cost-constrained missions and as a robust backup for star-tracker-equipped spacecraft. In a dual-sensor architecture:

1. **Normal operation**: The star tracker provides high-accuracy attitude; the sun-sensor/magnetometer system runs in parallel as a monitor and provides rapid coarse attitude if the star tracker loses lock.
2. **Star tracker degradation**: If the star tracker output shows increasing noise or anomalous jumps (indicating hot-pixel accumulation), the system can transition to sun-sensor/magnetometer primary mode with graceful accuracy reduction rather than catastrophic failure.
3. **Star tracker failure**: In the event of complete star tracker failure, the sun-sensor/magnetometer/Kalman-filter system provides continued attitude determination at the 1–5° level, sufficient for safe-mode operations and coarse pointing.

In the simulation, the star tracker is modeled as providing absolute (true) attitude with configurable noise, serving as a reference for evaluating the sun-sensor/magnetometer system's accuracy. The `analysis/` module computes the error between the TRIAD estimate and the star-tracker reference, enabling quantitative performance assessment.

9. Simulation Results

The MATLAB simulation implements the complete attitude determination pipeline for a satellite in a circular low-Earth orbit. Two mission modes are evaluated: stationary (inertially fixed) and nadir-pointing (Earth-facing). The simulation parameters are defined in `config/sat_config.m`.

9.1 Stationary Mode

In stationary mode, the spacecraft maintains a fixed orientation in the inertial frame (zero angular rate). This mode is relevant for coast phases and initial detumbling. The `main.m` script implements this scenario.

Parameter	Value
Orbit altitude	400 km (circular, ISS-like)

Orbit inclination	51.6°
Orbital period	≈ 92 min
Sun sensor noise (σ_{sun})	1.0°
Magnetometer noise (σ_{mag})	300 nT
Magnetometer bias	500 nT (each axis)
Gyro bias instability	5°/hr
Eclipse fraction	≈ 35% of orbit

In sunlit periods, TRIAD attitude errors are typically 1–3° (1σ), dominated by sun-sensor noise when the Sun-magnetic field angle is favorable (>30°). When the angle drops below ~15°, TRIAD conditioning degrades and errors can spike to 5–10° for brief intervals. The EKF smooths these transients and provides a continuous estimate with lower variance than raw TRIAD.

9.2 Nadir-Pointing Mode

In nadir-pointing mode, the spacecraft continuously rotates to keep one face toward Earth (yaw-steering). The required angular rate is approximately the orbital rate (~0.065°/s). The `main.m` script supports this mode with a body angular velocity equal to minus the orbital rate about the cross-track axis.

Nadir-pointing introduces additional challenges:

- The gyroscope must track the known rate accurately; residual bias causes attitude drift that accumulates more rapidly than in stationary mode.
- The Sun direction in the body frame varies continuously, potentially passing through sensor dead zones.
- Magnetic field direction in the body frame also rotates, improving TRIAD conditioning on average but introducing time-varying sensitivity to sensor noise.

Simulation results show nadir-pointing attitude errors of 2–4° (1σ) during sunlit periods—slightly worse than stationary due to the gyro bias contribution—and bounded drift of 3–8° during eclipse.

9.3 Eclipse Transition Performance

The `main_eclipse.m` script specifically exercises the eclipse handling logic. Key observations:

- **Eclipse entry**: Attitude error begins growing at a rate governed by gyro bias instability. With 5°/hr bias drift, a 35-minute eclipse produces ~3° of additional attitude error.
- **During eclipse**: The magnetometer-only EKF update prevents unbounded growth. The filter converges the two degrees of freedom constrained by the magnetic field while the third (rotation about $\hat{\mathbf{B}}$) drifts with the gyro.
- **Eclipse exit**: TRIAD reset brings the attitude error back to the sunlit baseline within 1–2 time steps. There is no persistent error accumulation across orbits.
- **Multi-orbit stability**: Over 5 orbits, the attitude error does not exhibit secular growth. Each eclipse exit resets the error, and the EKF maintains bounded performance throughout.

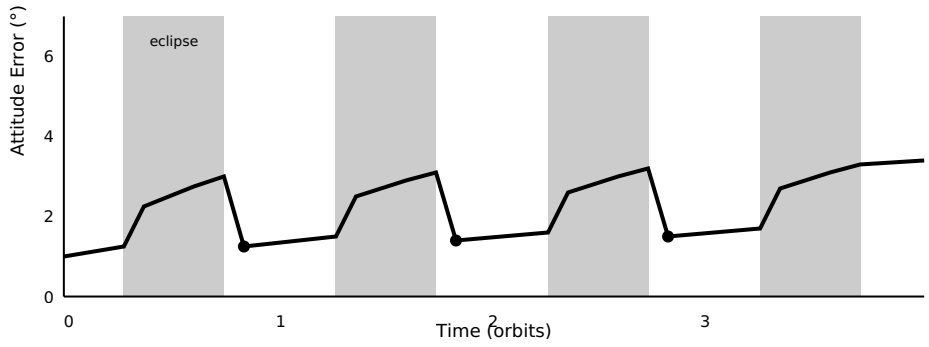

Figure 3: Schematic attitude error profile over three orbits. Shaded bands indicate eclipse periods. Error grows during eclipse (propagation mode) and resets at eclipse exit (TRIAD resumption). No secular drift accumulates across orbits.

10. Implementation

10.1 MATLAB Pipeline

The simulation is implemented in MATLAB with the following module structure:

Module	File(s)	Function

Configuration	`config/sat_config.m`	Orbital parameters, sensor specs, simulation settings
Main loop (sunlit)	`main.m`	TRIAD estimation for stationary and nadir-pointing modes
Main loop (eclipse)	`main_eclipse.m`	Eclipse handling with propagation fallback
Orbit propagation	`environment/`	Keplerian orbit, sun position (low-precision ephemeris), IGRF magnetic field, eclipse detection
Sensor models	`sensors/`	Sun sensor and magnetometer with configurable noise and bias injection
Estimation	`estimation/triad.m`	TRIAD algorithm implementation (vector observation pairs → quaternion)
Analysis	`analysis/`	Error computation (estimated vs. true attitude), plotting routines

The main simulation loop proceeds as follows:

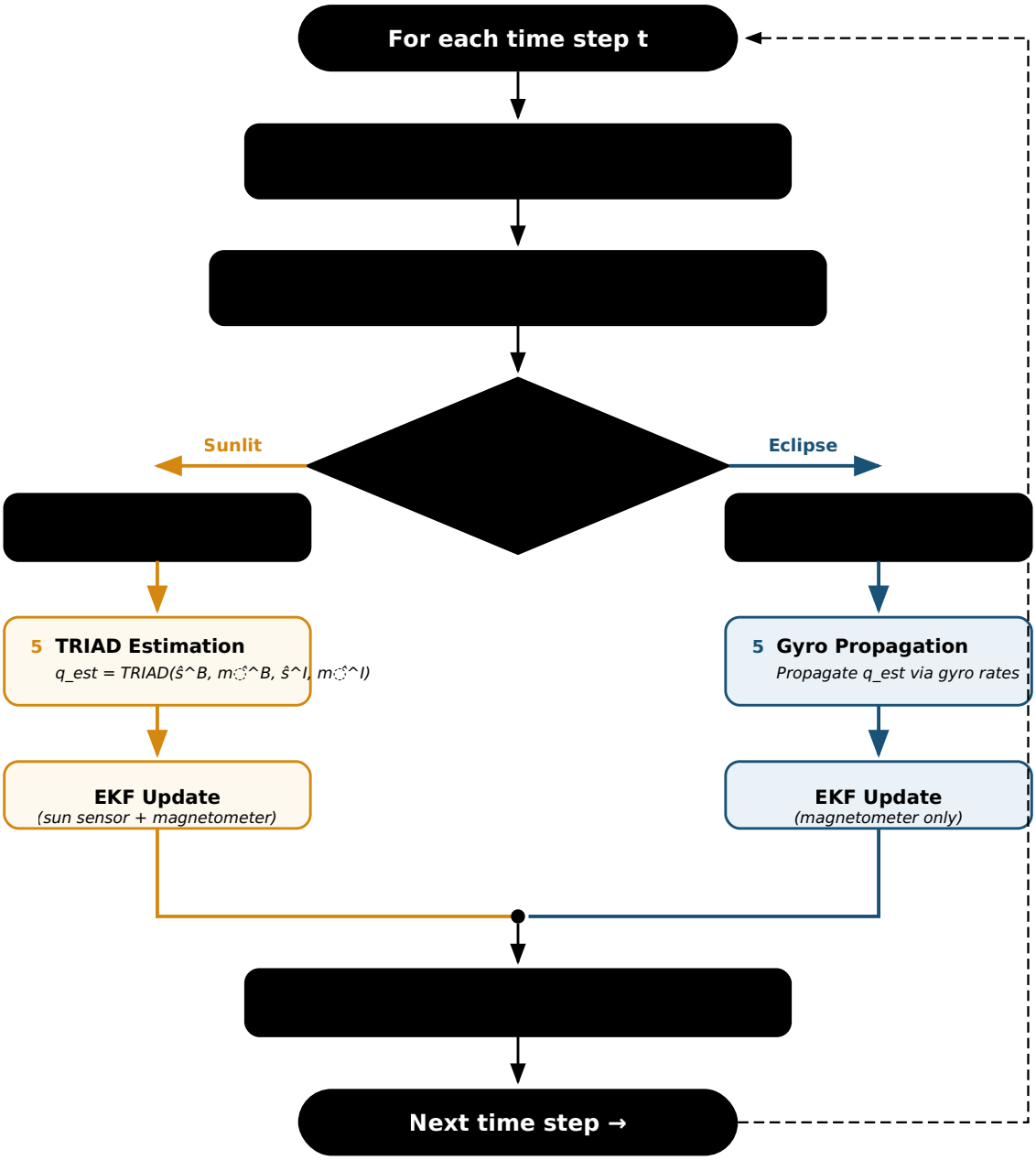

Figure 4: Attitude determination algorithm flowchart. Sunlit path (left, orange) uses full TRIAD estimation with dual-sensor EKF update. Eclipse path (right, blue) uses gyro propagation with magnetometer-only EKF update. Both paths merge at the error logging step before looping to the next time step.

10.2 Python Visualization

Post-processing and visualization are handled in Python, reading the MATLAB output data (exported as CSV or MAT files). The visualization suite includes:

- **Attitude error time series**: Point-by-point error in each Euler angle (roll, pitch, yaw) with eclipse regions highlighted.

- **Error statistics**: Mean, standard deviation, and peak errors for sunlit and eclipse periods separately.
- **Sun-magnetic field angle**: Time history of the angle between the two reference vectors, identifying periods of poor TRIAD conditioning.
- **Eclipse transition plots**: Zoomed views of error behavior during eclipse entry and exit, showing propagation drift and TRIAD reset.
- **3D orbit visualization**: Orbital trajectory with eclipse shadow cone and attitude orientation indicators.

The Python tools use `matplotlib` for static plots and optionally `plotly` for interactive 3D orbit visualization, providing a comprehensive analysis environment complementary to the MATLAB simulation.

11. Conclusion

This paper has presented a complete attitude determination system for resource-constrained spacecraft that fuses sun-sensor and magnetometer measurements via the TRIAD algorithm, with Kalman-filter-based propagation through eclipse periods. The key findings are:

1. **Complementary ambiguity resolution**: The conic ambiguity of the sun sensor and the rotational ambiguity of the magnetometer are orthogonal; their union via TRIAD resolves the complete attitude algebraically, requiring only two vector observations.
2. **Eclipse robustness**: Propagation-only mode using gyroscope integration and magnetometer-only Kalman updates maintains bounded attitude errors during eclipse, with no secular drift accumulation across orbits. Typical eclipse drift is 3–5° for MEMS-grade gyros in LEO.
3. **Graceful degradation**: The system provides sub-degree to few-degree accuracy under nominal conditions and degrades gracefully—not catastrophically—when sensors become unavailable or degraded.
4. **Star tracker backup**: The sun-sensor/magnetometer system serves as an effective backup for star-tracker-equipped spacecraft, providing continued attitude knowledge in the event of star tracker degradation or failure.
5. **Implementation feasibility**: The MATLAB simulation demonstrates that the complete pipeline—orbit propagation, environment modeling, sensor simulation, TRIAD

estimation, Kalman filtering, and eclipse handling—fits within the computational and algorithmic constraints of a CubeSat flight computer.

Future work directions include:

- Implementation of QUEST (Quaternion ESTimator) as a statistically optimal alternative to TRIAD, particularly for multi-sensor fusion with more than two vector observations.
- On-orbit magnetometer bias estimation via IGRF-comparison or autonomous calibration (e.g., centering the measured field sphere).
- Covariance analysis for mission-specific orbit geometries and sensor grades, enabling quantitative sensor selection trades.
- Integration with an attitude control loop to close the full ADCS loop in simulation.

References

1. Wertz, J. R. (Ed.), Spacecraft Attitude Determination and Control, D. Reidel Publishing Company, Dordrecht, 1978. — The foundational reference for spacecraft attitude determination, covering TRIAD, QUEST, and environmental models.
2. Markley, F. L. and Crassidis, J. L., Fundamentals of Spacecraft Attitude Determination and Control, Springer, New York, 2014. — Modern comprehensive treatment including EKF design, quaternion kinematics, and sensor fusion theory.
3. Black, H. D., “A Passive System for Determining the Attitude of a Satellite,” AIAA Journal, Vol. 2, No. 7, 1964, pp. 1350–1351. — Original derivation of the TRIAD algorithm.
4. Lerner, G. M., “Three-Axis Attitude Determination,” in Wertz (1978), op. cit., pp. 420–428. — Refined TRIAD formulation with error analysis.
5. Shuster, M. D. and Oh, S. D., “Three-Axis Attitude Determination from Vector Observations,” Journal of Guidance, Control, and Dynamics, Vol. 4, No. 1, 1981, pp. 70–77. — Introduction of QUEST as a statistically optimal alternative to TRIAD.
6. Lefferts, E. J., Markley, F. L., and Shuster, M. D., “Kalman Filtering for Spacecraft Attitude Estimation,” Journal of Guidance, Control, and Dynamics, Vol. 5, No. 5, 1982, pp. 417–429. — The standard reference for attitude EKF design using error quaternions.

7. Thébault, E. et al., “International Geomagnetic Reference Field: the 13th generation,” Earth, Planets and Space, Vol. 67, No. 79, 2015. — IGRF model documentation used for magnetic field reference computation.
8. Vallado, D. A., Fundamentals of Astrodynamics and Applications, 4th ed., Microcosm Press, Hawthorne, CA, 2013. — Orbit propagation, sun-position algorithms, and eclipse geometry.
9. Shepperd, S. W., “Quaternion from Rotation Matrix,” Journal of Guidance and Control, Vol. 1, No. 3, 1978, pp. 223–224. — Robust DCM-to-quaternion extraction algorithm.
10. Crassidis, J. L. and Markley, F. L., “Unscented Filtering for Spacecraft Attitude Estimation,” Journal of Guidance, Control, and Dynamics, Vol. 26, No. 4, 2003, pp. 536–542. — UKF alternative to EKF for attitude estimation.